

Research Article

Spatial Proximity and Relative Distribution of Tumor-Infiltrating Lymphocytes and Macrophages Predict Survival in Melanoma

Francesco De Logu^a, Filippo Ugolini^b, Luigi Francesco Iannone^a, Sara Simi^a, Vincenza Maio^b, Vincenzo de Giorgi^c, Anna Maria di Giacomo^d, Clelia Miracco^e, Antonio Cossu^f, Giuseppe Palmieri^g, Mario Mandalà^h, Daniela Massi^{b,*}

^a Department of Health Sciences, Section of Clinical Pharmacology and Oncology, University of Florence, Florence, Italy; ^b Department of Health Sciences, Section of Pathological Anatomy, University of Florence, Florence, Italy; ^c Department of Health Sciences, Section of Dermatology, University of Florence, Florence, Italy; ^d Medical Oncology and Immunotherapy, Center for Immuno-Oncology, University of Siena, Siena, Italy; ^e Unit of Pathological Anatomy, Department of Medicine, Surgery, and Neurosciences, University of Siena, Siena, Italy; ^f Section of Pathology, Department of Medical, Surgical and Experimental Sciences, University of Sassari, Italy; ^g Unit of Cancer Genetics, Institute of Genetic and Biomedical Research (IRGB), National Research Council (CNR), Sassari, Italy; ^h Oncology Unit, Department of Medicine and Surgery, University of Perugia, Perugia, Italy

ARTICLE INFO

Article history:

Received 16 March 2023
Revised 13 September 2023
Accepted 7 October 2023
Available online 13 October 2023

Keywords:

primary cutaneous melanoma
prognosis
spatial proximity
tumor-associated macrophages
tumor-infiltrating lymphocytes
tumor microenvironment

ABSTRACT

Tumor microenvironment plays a crucial role in primary cutaneous melanoma (CM) progression. Although the role of tumor-infiltrating lymphocyte (TIL) density has been known for a long time, its spatial distribution and impact with or without tumor-associated macrophages (TAMs) remain controversial. Herein, we investigated spatial proximity between tumor cells and immune cells in 113 primary CM and its correlation with disease-free (DFS) and overall survival (OS). The study cohort included clinical stage II ($n = 79$) and stage III ($n = 34$) primary CM with a Breslow thickness of >2 mm (with a median age of 64 years, including 72 men and 41 women). In univariate models, patients with SOX10+ melanoma cells with high proximity to CD8+ TILs in a 20 μ m radius showed longer DFS (hazard ratio [HR], 0.58; 95% CI, 0.36–0.93; $P = .025$) and OS (HR, 0.55; 95% CI, 0.32–0.92; $P = .023$). Furthermore, at multivariate combined analysis, patients with SOX10+ melanoma cells with high proximity to CD8+ TILs or low proximity to CD163+ TAMs in a 20 μ m radius showed an increased OS (aHR, 0.37; 95% CI, 0.14–0.96; $P = .04$) compared with melanoma patients with low proximity to CD8+ TILs or high proximity to CD163+ TAMs. In a subgroup analysis including 92 patients, a significant negative impact on DFS (aHR, 4.49; 95% CI, 1.73–11.64; $P = .002$) and OS (aHR, 3.97; 95% CI, 1.37–11.49; $P = .01$) was observed in sentinel lymph node (SLN)-negative patients with a high proximity of CD163+ TAMs to CD8+ TILs. These findings could help identify high-risk patients in the context of thick melanoma and a negative SLN. Our study suggests the importance of quantifying not only the density of immune cells but also the individual and combined relative spatial distributions of tumor cells and immune cells for clinical outcomes in SLN-negative primary CM patients.

© 2023 THE AUTHORS. Published by Elsevier Inc. on behalf of the United States & Canadian Academy of Pathology. This is an open access article under the CC BY license (<http://creativecommons.org/licenses/by/4.0/>).

These authors contributed equally: Francesco De Logu and Filippo Ugolini.

* Corresponding author.

E-mail address: daniela.massi@unifi.it (D. Massi).



Introduction

Cutaneous melanoma (CM) is an aggressive disease, and it is one of the major causes of cancer-related death. About 90% of skin cancer mortality is caused by CMs.¹ Accurate prediction of prognosis is important to determine the need for further investigations, select appropriate management, and assign the risk status of melanoma patients.² In primary CM, Breslow thickness, ulceration, and sentinel lymph node (SLN) assessment are considered independent prognostic factors.³ Recently, accumulating evidence suggested that melanoma growth is also influenced by the host immune response and inflammatory cells within the tumor micro-environment (TME).⁴ Indeed, the presence of tumor-infiltrating lymphocytes (TILs) in primary CM has been associated with a favorable prognosis, and the correlation between brisk TIL and improved survival of primary CM patients has been reported in multiple studies.⁵⁻⁹ In particular, primary CM patients with high-density CD8+ TILs cells showed more than three times 5-year survival compared with the low-density group.¹⁰ The positive prognostic role of CD8+ TILs has also been confirmed with digital image analysis quantification as total intratumoral cell density.^{11,12}

In contrast, the prognostic role of tumor-associated macrophage (TAM) infiltration in primary CM remains still unclear. TME is characterized by a wide range of molecule products both from malignant and stromal cells, and TAMs respond to this microenvironmental complexities with a phenotype switch in M1, classically activated and tumoricidal macrophages, or M2 alternatively activated protumorigenic macrophages.^{13,14} However, in primary CM, some studies have observed no prognostic role,^{10,15} whereas other studies showed that the numbers of total TAMs CD68+ and M2 phenotype CD163+ cell quantification were correlated with unfavorable outcomes, maintaining their role controversial.^{14,16,17}

Technological advances using digital image analysis tools allow a precise and reproducible quantitation of immune populations within the TME of primary CM.¹⁸ To date, there are only a few studies that applied computational pathology methods to quantify and characterize the spatial distribution of TIL and TAM populations in primary CM.^{11,12,19} The spatial distribution of tumor cells relative to immune cells and the spatial relation between different immune cells may influence melanoma disease progression, and additional computational parameters obtained by spatial proximity analysis could help better stratify the cohorts of primary CM patients.^{11,19} The relative spatial proximity distribution of tumor cells and TILs and TAMs and their association with survival in primary CM melanoma remain largely unexplored.

Herein, we explored for the first time the spatial distribution of melanoma tumor cells (SOX10+) and immune CD8+ and CD163+ cells in primary CM tissues using validated multiplex brightfield immunohistochemistry (IHC) protocols.²⁰ The relative spatial distributions were expressed as average distance, average number, and proximity distribution between tumor and immune cells. These measurements were quantified and correlated with clinicopathological characteristics, DFS, and OS. In particular, we showed a correlation between the proximity of SOX10+ cells to immune cells, SOX10+ cells proximity within immune cells (100 and 20 μ m radius), indirect proximity, and relative spatial distribution between CD8+ and CD163+ cells and clinical outcomes.

Materials and Methods

Patient Characteristics

The cohort ($n = 113$) included patients with clinical stages II–III intermediate/thick primary CM with a Breslow thickness of >2 mm diagnosed, treated, and followed up prospectively in four Italian centers (University of Florence, Florence, Italy; University of Sassari, Sassari, Italy; University Hospital of Siena, Siena, Italy; and Papa Giovanni XXIII Cancer Center Hospital, Bergamo, Italy) from 1994 to 2020. The clinical and histopathological parameters extracted from the database included the following: sex, date of birth, date of diagnosis of CM, histotype, anatomical site, Breslow thickness, ulceration, mitotic rate, SLN status, TILs, and follow-up including the dates of relapse and death. Only primary CM samples previously classified as TILs brisk or nonbrisk were included in the study; however, primary CM samples with TILs absent were excluded.

Tissue Samples

Formalin-fixed paraffin-embedded (FFPE) tissue sections, 3 μ m in thickness, were stained with hematoxylin & eosin and reviewed to confirm the histopathological diagnosis and assess tissue quality control.

Immunohistochemistry

For SOX10/CD8/CD163 multiplex protocol, sections were deparaffinized in EZ prep (950-102; Ventana), and antigen retrieval was achieved with cell-conditioning solution 1 pH 8.2 (950-124; Ventana). Sections were incubated with the following primary antibodies: anti-SOX10 (#760-4968, rabbit monoclonal, clone SP267, ready-to-use, Ventana Medical Systems), anti-CD8 (#790-4460, rabbit monoclonal, clone SP57, ready-to-use, Ventana Medical System), and anti-CD163 (#05973929001, mouse monoclonal, clone MRQ-26, ready-to-use, Ventana Medical Systems). The signal was developed with antimouse or antirabbit Alk Phos, and antirabbit HRP was coupled with the following chromogens: DISC. GREEN HRP Kit (#08478295001, ready-to-use, Ventana Medical Systems), DISC. YELLOW Kit (#076984 45001, ready-to-use, Ventana Medical Systems), and DISC. Chromomap RED (#05266653001, ready-to-use, Ventana Medical Systems). Sections were counterstained with hematoxylin II (#05277965001, ready-to-use, Ventana Medical Systems).

Image Analysis

Stained tissue sections were digitally scanned at $\times 400$ magnification with the Aperio AT2 platform (Leica Biosystems) into whole slide digital images. Each SVS format file was imported into HALO Link (Indica Labs) image management system. Two expert pathologists (D.M., V.M.) drew the image annotations of the whole surface and margins of primary CM. According to ITWG recommendations, the whole tumor area was defined as the area containing invasive tumors, including the invasive tumor borders. Detection of immune-stained positive cells was performed using HALO Multiplex IHC analysis software version v3.1.1076.308 (Indica Labs), based on cytonuclear features such as stain intensity, size, and roundness (nuclear contrast threshold 0.453,

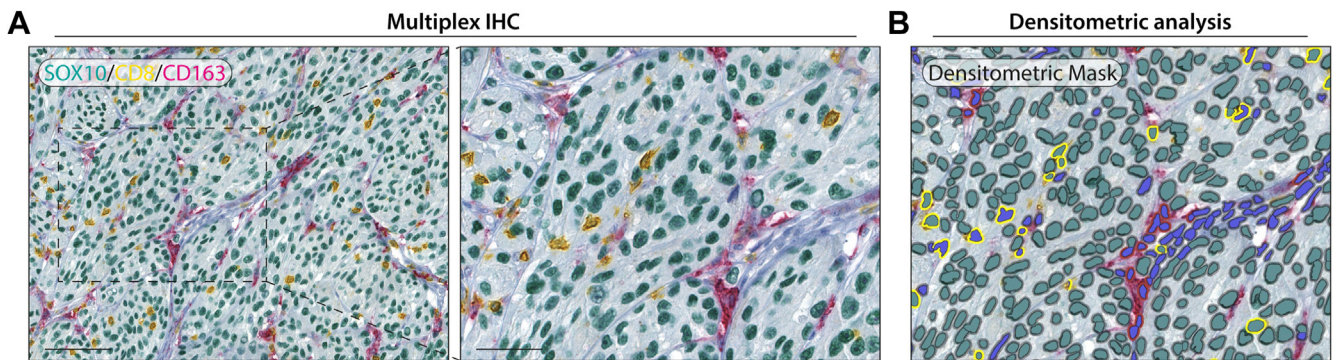


Figure 1.

Representative triple-labeling for SOX10/CD8/CD163 of melanoma tissue (A), and counterstain was performed with hematoxylin. Magnification: 200 \times and 400 \times (scale bar: 100 and 50 μ m). Representative HALO densitometric recognition mask of SOX10/CD8/CD163 expression (B).

minimum optical nuclear density 0.172, and nuclear segmentation aggressiveness 0.278, respectively) for CD8, CD163, and SOX10 (Fig. 1A). For absolute density, data were expressed as cellular density (ie, the number of positive cells divided by the mm² of the annotation layer area).

The software automatically excludes melanin pigment and tissue gaps from the analysis, and the settings were set up to include the full range of staining intensity (from weak to strong; Fig. 1B). Evaluation of the quality of the analysis performed with HALO software was obtained by comparing the data calculated automatically and manually by expert pathologists (V.M. and D.M.). Therefore, regions of interest of 15 μ m diameter in random position inside the tumor area, on each sample, were considered. For each region of interest, we evaluated the number of CD8+, CD163+, and SOX10+ cells using both software and manual counting. Obtained values were used to calculate the Sørensen–Dice coefficient of similarity.²¹ The results reached Sørensen–Dice coefficients of 0.93 for CD8+, 0.87 for CD163+, and 0.73 for SOX10+ cell evaluations.

Proximity analysis was defined as the distance of tumor cells distributed within a specific radius from the nuclear center of any given immune cell. We set up the following three different proximity analyses: (i) average distance, the mean distance of all SOX10-positive cells to CD8 or CD163-positive cells calculated in all the intratumoral area; (ii) average number, the absolute number of SOX10-positive cells to CD8- or CD163-positive cells calculated in all the intratumoral area; and (iii) cells proximity within 0–20 (μ m), the number of SOX10-positive cells to CD8- or CD163-positive cells calculated in the range of 0–20 μ m in all the intratumoral area normalized for the area (expressed as cells/mm²). However, the same settings were used for the analyses between CD8 and CD163 immune cells.

We investigate whether the number of SOX10+ cells within a specific distance to CD8+ TILs and/or CD163+ TAMs would impact DFS and OS and within different SLN statuses. Considering previous studies on melanoma,^{11,12} we investigated the proximity of SOX10+ cells within a 0–20 μ m radius to any given CD8+ TILs and/or CD163+ TAMs.

Statistical Analysis

Considering the exploratory design, the sample size was not based on any statistical considerations, and we included all patients available at the time of analysis. However, the sample size is in line with or larger than that of previous studies.^{11,19,22}

Each tumor cell was evaluated as a continuous variable (mean \pm SD or median [Q1–Q3]), and then, the high- and low-proximity

values were determined based on the median. Therefore, DFS was defined as the time between diagnosis and disease relapse or death from any cause (ie, DFS events are the events of relapse or/and death). Additionally, OS was defined as the time between diagnosis and death from any cause. Patients who had not experienced relapse or had not died were censored at the date of their last follow-up visit. Crude Kaplan–Meier log-rank analyses were performed to determine the associations between cell distances and DFS or OS. The overall density of SOX10+ and immune cells and the high and low proximities of SOX10+ cells to immune cells were determined based on the median distance. The optimal cutoffs for Kaplan–Meier analyses were also determined using the median.^{22,23} The independent prognostic values of proximity were estimated using univariate and multivariate Cox proportional hazard regression models and expressed as hazard ratio (HR), adjusted HR (aHR), and 95% CI. The multivariate Cox model was adjusted for Breslow thickness, ulceration, mitotic rate/mm², and SLN status. The χ^2 test of homogeneity and the Mann–Whitney *U* test have been used as appropriate. Immune cells have been also combined using SOX10+ cells in proximity to both CD8+ TILs and CD163+ TAMs. A *P* value <.05 was considered statistically significant, as otherwise specified due to Bonferroni correction. All the data were analyzed using SPSS software version 26.0 (IBM Corp. SPSS Statistics).

Results

Cohort Characteristics

This study included FFPE of primary CM samples from 113 patients. The median age was 60.5 years (SD 16.8), and 72 patients (63.7%) were men. Overall, 62 patients (54.9%) relapsed, 60 patients (53.1%) died, and 71 patients (62.8%) relapsed and died. The median OS and DFS were 102 months (95% CI, 60.45–143.54) and 46 months (95% CI, 28.01–63.98), respectively. Finally, among 92 patients (92/113, 81.4%) who underwent a SLN biopsy, 38 (41.3%) were SLN-positive. For 21 patients (21/113; 18.6%), the SLN status was unknown (Table 1).

Analysis Between Tumoral Cells (SOX10+) and Immune Cells (CD8+ TILs and CD163+ TAMs)

Average Distance of Tumor Cells to Immune Cells

Detection of positive cells was performed using HALO Multiplex IHC analysis software (Fig. 1A, B). To evaluate whether the

Table 1
Demographic and clinical features of study patients

	Patients (n = 113)
Age (y), mean (SD)	60.5 (16.8)
Male sex, n (%)	72 (63.7)
Tumor site, n (%)	
Limbs	43 (38.1)
Trunk	55 (47.8)
Head/neck	10 (8.8)
Acral	6 (5.3)
Histotype n, (%)	
Superficial Spreading Melanoma	60 (53.1)
Nodular Melanoma	46 (40.7)
Acral Melanoma	6 (5.3)
Lentigo Maligna Melanoma	1 (0.9)
Breslow thickness (mm), mean (SD)	5.2 (4.48)
Mitotic rate/mm ² , mean (SD)	8.5 (7.5)
Ulceration, n (%)	
Present	84 (74.3%)
Absent	29 (25.7%)
TILs, n (%)	
Brisk	19 (16.8)
Nonbrisk	94 (83.2)
SLN status, n (%)	
SLN status available, n (%)	92 (81.4)
SLN positive ^a , n (%)	38 (41.3)

Percentages are on column total if not otherwise specified. SD, standard deviation; SN, sentinel lymph node; TIL, tumor-infiltrating lymphocytes.

^a On SN status available.

relative spatial distribution of SOX10+ melanoma cells and CD8+TILs and CD163+ TAMs could predict prognosis, first, we calculated the mean distance from melanoma cells to each immune cell (Supplementary Fig. S1A, B). The mean distances of SOX10+ cells to CD8+ TILs and CD163+ TAMs were 102.57 μm (±76.2) and 44.05 μm (±26.2), respectively (Supplementary Fig. S1C). The high and low proximities of SOX10+ cells to immune cells were determined based on the median distance. Therefore, OS was not influenced by SOX10+ cells high proximity to CD8+ cells, whereas OS was decreased by SOX10+ cells high proximity to CD163+ cells (Supplementary Fig. S1D, E; Table S1). Then, we evaluated SOX10+ cells proximity to both CD8+ and CD163+ cells (according to median: SOX10+ cells near (high proximity) or far (low proximity), near to CD8+ and far to CD163+ cells and vice versa). Although the crude survival distributions of all groups were not statistically significantly different (Supplementary Fig. S1F), exploratively pairwise log-rank comparisons were conducted. A significantly longer OS was observed in patients with SOX10+ cells high proximity to CD8+TILs/low proximity to CD163+TAMs compared with patients with SOX10+ cells low proximity to CD8+ TILs/high proximity to CD163+ TAMs expressed as average distances (high–low vs low–high, $\chi^2 = 7.741, P = .005; P < .0125$; Supplementary Fig. S1F). Accordingly, selecting and comparing only the groups that demonstrate significant differences in crude KM pairwise analysis, a numerically longer OS was found in multivariate regression analysis comparing high–low vs low–high (HR, 0.24; 95% CI, 0.08–0.71; $P = .01$; and aHR, 0.33; 95% CI, 0.10–1.05; $P = .06$).

Tumor Cells Proximity From Immune Cells Within 0–20 μm

To investigate the clinical impact of a close melanoma-immune cell contact, we evaluated the number of SOX10+ cells using a small radius (0–20 μm) from immune cells (Fig. 2A, B). SOX10+ cells within 20 μm are quantified as proximity and reported as

cells per mm². The mean SOX10+ cells to CD8+ and CD163+ cells in 0–20 μm were 555.11 (605.4) and 1184.21 (850.1), respectively (Fig. 2C). The high and low proximities of SOX10+ cells to immune cells were determined based on the median distance. Intratumoral absolute density (number of CD8+, CD163+, or SOX10+ cells without range definition) did not recapitulate the proximity categorization (Supplementary Fig. S2). Indeed, a remarkable percentage of patients have a discordant pattern considering the absolute density of immune cells (25.7% and 11.5% for CD163+ and CD8+ density, respectively) or the absolute density of tumor cells (43.4% for SOX10+CD163+ and 38.1% SOX10+CD8+). Therefore, we calculated DFS and OS using proximity parameters, and then, we calculated survival with density parameters to evaluate possible correspondence.

In the proximity analyses, patients with SOX10+ cells high proximity to CD8+ TILs in a 0–20 μm radius showed longer DFS and OS (Fig. 2D, F) at univariate but not multivariate analyses (Table 2). No significant differences for patients with SOX10+ cells high proximity to CD163 TAMs in a 0–20 μm radius in DFS and OS (Fig. 2E, G) were observed (Table 2).

The crude survival distributions for the 4 proximity combinations (high–high, high–low, low–high, and low–low proximity) were significantly different for DFS ($\chi^2 = 8.375, P = .039$) and OS ($\chi^2 = 9.939, P = .019$; Fig. 2H, I). In the related pairwise comparison, patients with SOX10+ melanoma cells with high proximity to CD8+ TILs or low proximity to CD163+ TAMs showed longer OS compared with patients with SOX10+ melanoma cells with low proximity to CD8+ TILs or high proximity to CD163+ TAMs ($\chi^2 = 7.485, P = .006, Fig. 2I$). This influence was also observed in univariate and multivariate models reported in Table 2. Moreover, patients with SOX10+ melanoma cells with high proximity to CD8+ TILs/high proximity to CD163+ TAMs showed longer DFS compared with patients with SOX10+ melanoma cells with low proximity to CD8+ TILs/high proximity to CD163+ TAMs at univariate but not multivariate regressions (Table 2). Other survival distributions were not statistically significant according to pairwise P correction ($P < .0125$) and in Cox regressions.

On the other hand, to strengthen the finding that proximity is not just a different expression of absolute density, we performed survival analyses considering the absolute density of SOX10+, CD8+, CD163+ (Supplementary Fig. S3A–F), and the combination of SOX10+CD8+ or SOX10+CD163 (Supplementary Fig. S4A–D) that did not recapitulate proximity results, with no significant results (Supplementary Table S2).

Analysis Between Immune Cells (CD8+ TILs and CD163+ TAMs)

A separate analysis between immune cells performed with the same analysis setting between SOX10+ cells and immune cells (ie, average distance, average number, and spatial proximity distribution of tumor cells within 0–20 μm) was carried out.

The average distances of CD8+ from CD163+ cells were 19.15 μm (±11.7) and 54.6 μm vice versa (±42.7; Fig. 3A). The high and low proximities of CD8+ cells from CD163+ cells and vice versa were determined based on the median distance.

Therefore, DFS and OS were not significantly reduced in patients with high proximity of CD8+ TILs to CD163+ TAMs (Fig. 3B; Table 3). Likewise, in patients with high proximity of CD163+TAMs to CD8+ TILs, DFS and OS have no definite pattern (Fig. 3C; Table 3). The average numbers of CD8+ cells within a 100-μm radius from CD163+ cells or vice versa were 1.39 (0.39) and 7.71 (5.88), respectively (Fig. 3D). However, DFS and OS were influenced by the average number of CD8+ TILs within a 100-μm

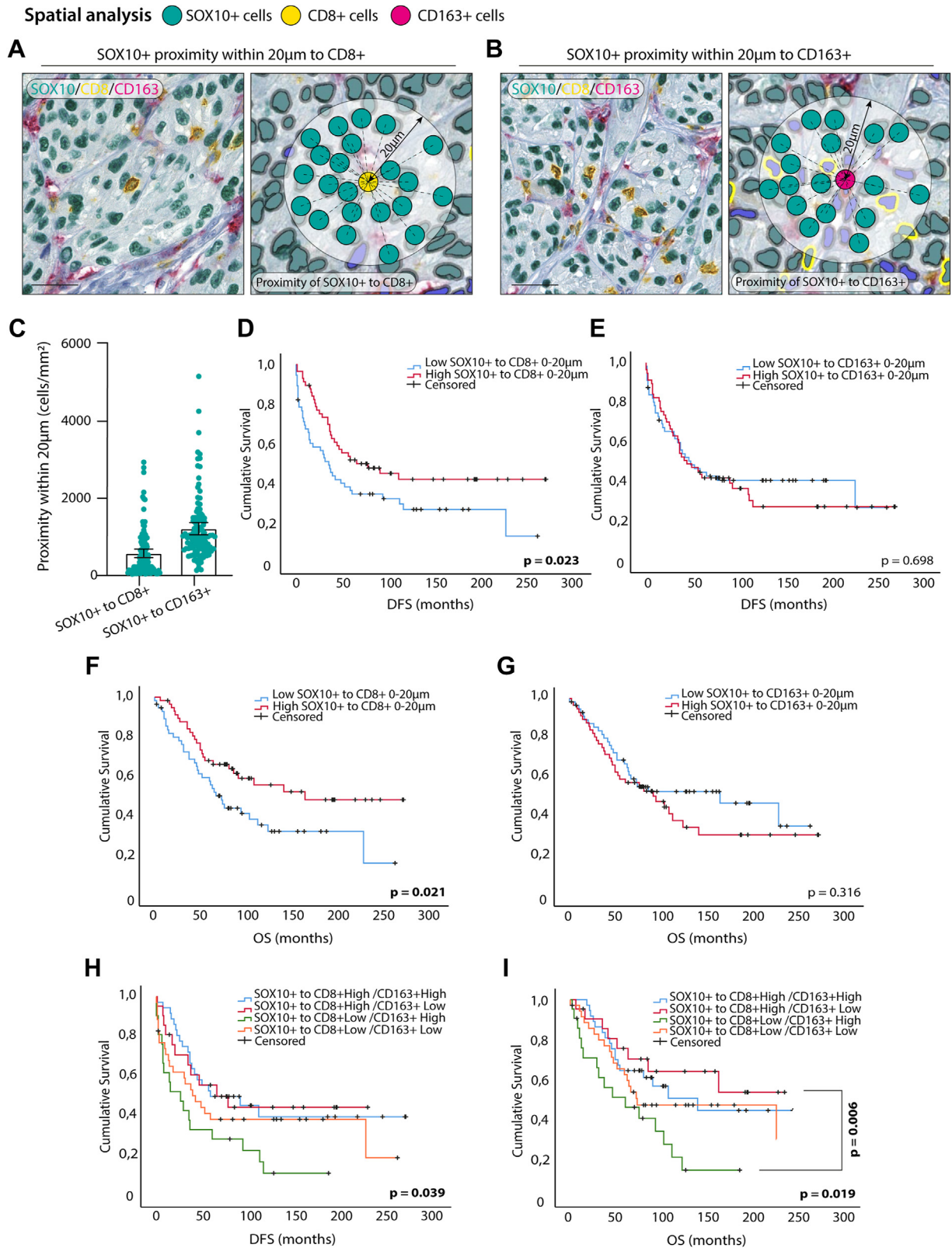


Figure 2.

Representative intercellular spatial distribution in melanoma tissue between SOX10+ cells and CD8+ (A) or CD163+ (B) cells within a 20 µm radius. Counterstain was performed with hematoxylin. Magnification: 400× (scale bar: 50 µm). Comparison between SOX10+ proximity within 20 µm to CD8+ and CD163+ cells (C), and every dot represents the mean distance of SOX10+ cells to immune cells for each patient. Crude Kaplan–Meier survival analyses of SOX10+ to CD8+ proximity within 20 µm (D, F) ($\chi^2 = 5.200$, $P = .023$ and log-rank $\chi^2 = 5.301$, $P = .021$, respectively) or SOX10+ to CD163+ proximity within 20 µm (E, G) ($\chi^2 = 1.51$, $P = .698$ and log-rank $\chi^2 = 1.00$, $P = .316$, respectively). Patients were divided into the high- and low-proximity groups, based on the median values, respectively. Combined SOX10+ cells proximity to both CD8+ and CD163+ cells according to median (high- and low-proximity groups) (H, I) ($\chi^2 = 8.375$, $P = .039$ and log-rank $\chi^2 = 9.939$, $P = .019$, respectively). Related pairwise comparison, high–low proximity patients showed longer OS compared with low–high proximity patients ($\chi^2 = 7.485$, $P = .006$). P values reflect the comparisons between 2 or 4 (H, I) groups by univariate analysis using the log-rank test.

Table 2
Cox regression analysis of prognostic factors for disease-free survival and overall survival with SOX10+ proximity to CD8+TILs and CD163+ TAMs in the 0–20 μm radius

	Disease-free survival				Overall survival			
	Univariable		Multivariable		Univariable		Multivariable	
	HR (95% CI)	P value	HR (95% CI)	P value	HR (95% CI)	P value	HR (95% CI)	P value
SOX10+ to CD8+ (high vs low)	0.58 (0.36–0.93)	.025 ^c	0.78 (0.47–1.31)	.35	0.55 (0.32–0.92)	0.02 ^c	0.69 (0.39–1.19)	.18
SOX10+ to CD163+ (high vs low)	1.09 (0.68–1.74)	.69	1.17 (0.72–1.89)	.52	1.29 (0.77–2.15)	0.31	1.45 (0.86–2.45)	.15
SOX10+ to combined CD8+ CD163+ ^a								
High–High	0.70 (0.38–1.29)	.25	0.92 (0.48–1.76)	.81	0.76 (0.39–1.47)	0.42	0.99 (0.50–1.96)	.97
High–Low	0.71 (0.34–1.46)	.35	0.90 (0.42–1.92)	.79	0.57 (0.25–1.31)	0.19	0.65 (0.27–1.52)	.35
Low–High	1.63 (0.87–3.04)	.12	1.48 (0.77–2.81)	.23	1.82 (0.93–3.56)	0.07	1.71 (0.87–3.35)	.11
SOX10+ to combined CD8+ CD163+ ^b								
High–Low	/	/	/	/	0.31 (0.13–0.75)	0.009 ^c	0.37 (0.14–0.96)	.04 ^c
High–High	0.44 (0.20–0.93)	.03 ^c	0.59 (0.25–1.41)	.24	/	/	/	/

Multivariable models adjusted for Breslow thickness, ulceration, mitotic rate, and sentinel lymph node.

^a Low–low used as reference.

^b Combining only high–low (OS) or high–high (DFS) and low–high (as reference); n = 42.

^c Statistically significant.

radius from CD163+ TAMs (Fig. 3E, G) and vice versa (Fig. 3F, H). In particular, high average numbers of CD8+ TILs to CD163+TAMs cells have a positive impact on DFS and OS in univariate but not multivariate models (Table 3). Inversely, high average numbers of CD163+ TAMs to CD8 TILs have a significant negative impact on DFS and OS in univariate but not multivariate models (Table 3).

The mean numbers of CD8+ cells within a 20 μm radius from CD163+ cells (Supplementary Fig. S5A, B) or vice versa were 329.88 (370.6) and 741.58 (741.4), respectively (Supplementary Fig. S5C). High proximity of CD8+ cells to CD163+ cells and vice versa has a not statistically significant impact on DFS and OS (Supplementary Fig. S5D–G; Table 3).

Regarding absolute intratumoral density, the survival analyses considering the combination of CD8+ CD163+ density did not mirror proximity analysis (Supplementary Fig. S4E, F; Table S2).

SLN Subgroup Analysis

A separate exploratory subgroup analysis in SLN-positive (n = 38) and SLN-negative (n = 54) groups (Table 1) performing the same analysis between SOX10+ cells and immune cells (ie, average distance, average number, and spatial proximity distribution of tumor cells within 0–20 μm) found no statistically significant results or a definite pattern. On the other hand, assessing the indirect proximity among CD8+ TILs and CD163+ TAMs, we demonstrated a significant difference in the average number of CD8+ cells to CD163+ cells and vice versa for both DFS and OS in SLN-negative but not in SLN-positive patients. In detail, the average numbers of CD8+ cells to CD163+ cells and CD163+ cells to CD8+ cells in 100 μm were 1.28 (0.18) and 8.22 (4.68) in SLN-positive patients, whereas the average numbers were 1.48 (0.48) and 6.94 (5.99) in SLN-negative patients, respectively.

A statistically significant difference in OS was found with the average number of CD8+ cells to CD163+ cells (Fig. 4E) and CD163+ cells to CD8+ cells (Fig. 4G) within 100 μm in SLN-negative patients but not in SLN-positive patients CD8+ to CD163+ (Fig. 4F) and CD163+ cells to CD8+ cells (Fig. 4H). In particular, in SLN-negative patients, high proximity of CD8+ cells to CD163+ cells has a positive impact on OS (aHR, 0.24; 95% CI, 0.08–0.67; P = .007; and aHR, 0.21; 95% CI, 0.06–0.63; P = .006), whereas high proximity of CD163+ cells to CD8+ cells has a significant negative impact on OS (aHR, 3.69; 95% CI, 1.31–10.38; P = .01; and aHR, 3.97; 95% CI, 1.37–11.49; P = .01; multivariate adjusted for ulceration, mitotic

rate, and Breslow thickness). No significant differences have been reported in the SLN-positive cohort. Regarding DFS, spatial distributions within 100 μm of CD8+ cells to CD163+ cells (Fig. 4A) or CD163+ cells to CD8+ cells (Fig. 4C) have a statically significant positive and negative impact on tumor relapse, respectively, in SLN-negative patients but not in SLN-positive patients (Fig. 4B, D). In particular, in SLN-negative patients, high proximity of CD8+ TILs within 0–100 μm to CD163+TAMs cells have a statistically significant positive impact on DFS (HR, 0.27; 95% CI, 0.11–0.68; P = .005; and aHR, 0.29; 95% CI, 0.11–0.75; P = .01). On the other hand, high proximity of CD163+ cells within 0–100 μm to CD8+ cells have a significant negative impact on DFS (HR, 4.13; 95% CI, 1.63–10.45; P = .003; and aHR, 4.49; 95% CI, 1.73–11.64; P = .002).

No differences have been reported for indirect distances between immune cells in SLN-positive or SLN-negative patients regarding average distance and spatial proximity distribution within 0–20 μm of each other.

Discussion

In the present study, we obtained the following 3 main results: (1) OS was significantly longer in melanoma patients with tumor cells with high proximity to CD8+ TILs/low proximity to CD163+ TAMs compared with those with tumor cells with low proximity to CD8+ TILs/high proximity to CD163+ TAMs in a radius of 0–20 μm; (2) high average number within 100 μm of CD8+ cells to CD163+ cells had a positive impact on OS, whereas high average number within 100 μm of CD163+ cells to CD8+ cells had a significant negative impact on OS in SLN-negative patients; and (3) in SLN-negative patients, high average numbers within 100 μm of CD8+ cells to CD163+ cells or CD163+ cells to CD8+ cells had a statistically significant positive and negative impact on tumor relapse, respectively.

The nature of melanoma immune cells relationship requires a comprehensive understanding of its microenvironmental complexities. In our previous study on absolute density and spatial distribution of immune cells in intermediate/thick primary CM,¹² we demonstrated that high CD8+ TILs density in the intratumoral area was correlated with a favorable patient outcome on digital image acquisition and quantitative analysis. Although statistical significance was not reached for absolute density analysis of CD8+ and CD163+ cells in these cohorts of patients, the survival results are in line with the previously published results,¹² confirming a

Spatial analysis ● CD8+ cells ● CD163+ cells

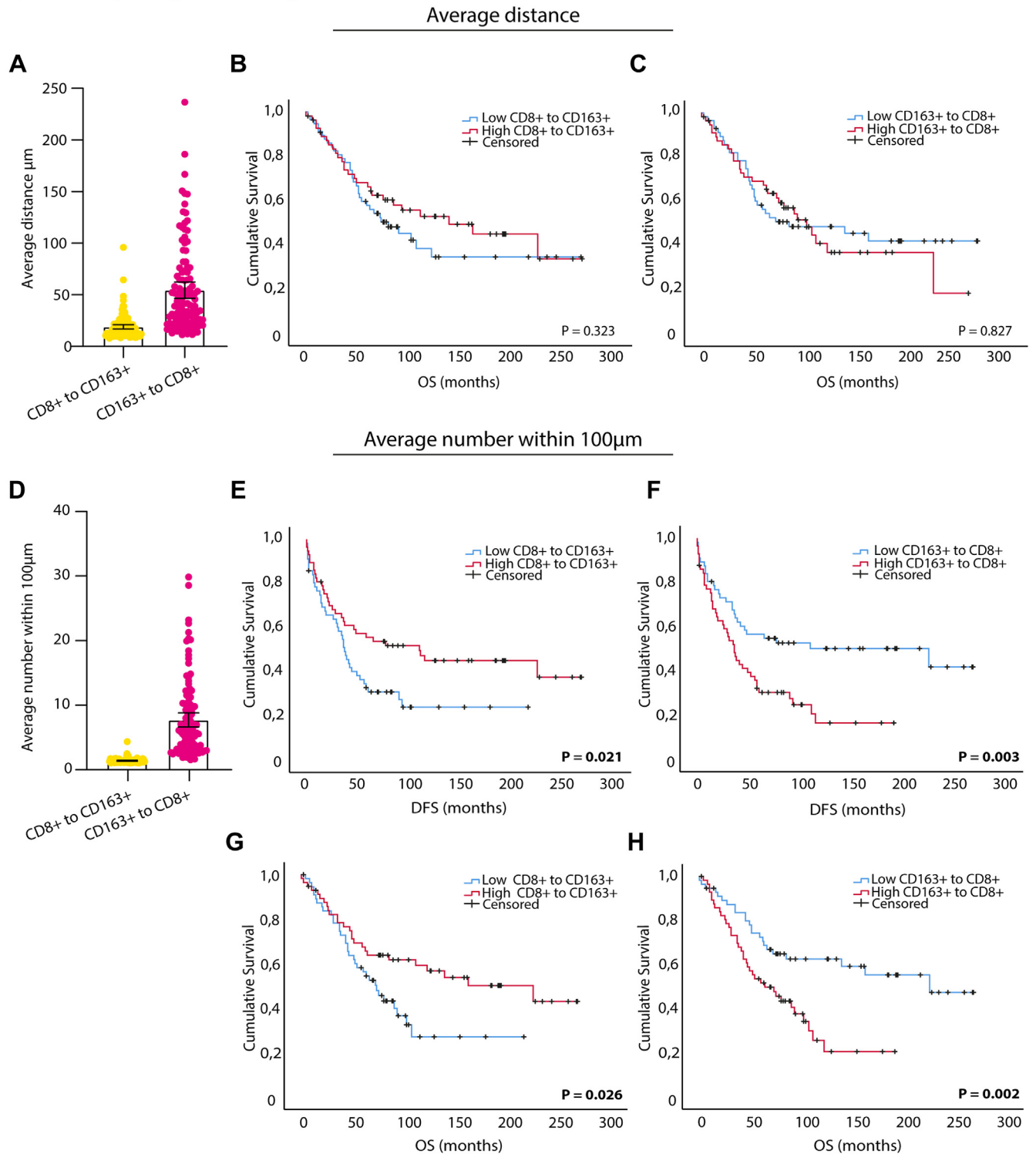


Figure 3.

Comparison between CD8+ to CD163+ or CD163+ to CD8+ average distance, and every dot represents the average distance of CD8+ to CD163+ cells and *vice versa* for each patient (A). Crude Kaplan–Meier survival analyses of CD8+ to CD163+ average distance (B) (log-rank $\chi^2 = 0.97$, $P = .323$) or CD163+ to CD8+ average distance (C) (log-rank $\chi^2 = 0.04$, $P = .827$). Comparison between CD8+ to CD163+ or CD163+ to CD8+ average number, and every dot represents the average number within 100 μm of CD8+ to CD163+ cells and *vice versa* for each patient (D). Crude Kaplan–Meier survival analyses of CD8+ to CD163+ average number (E, G) ($\chi^2 = 5.35$, $P = .021$ and log-rank $\chi^2 = 4.98$, $P = .026$, respectively) or CD163+ to CD8+ average number (F, H) ($\chi^2 = 8.58$, $P = .003$ and $\chi^2 = 9.48$, $P = .002$, respectively). Patients were divided into the high- and low-proximity groups, based on the median values, respectively. P values reflect the comparisons between 2 groups by univariate analysis using the log-rank test.

Table 3
Cox regression analysis of prognostic factors for disease-free survival and overall survival between average distance, average number in the 100 μm radius, and proximity distribution in the 0–20 μm radius of CD8+ TILs to CD163+TAMs and vice versa

	Disease-free survival				Overall survival				
	Univariable		Multivariable		Univariable		Multivariable		
	HR (95% CI)	P value	aHR (95% CI)	P value	HR (95% CI)	P value	aHR (95% CI)	P value	
Average distance ^a									
CD8+ to CD163+	1.47 (0.92–2.36)	.10	1.31 (0.79–2.17)	.28	1.29 (0.77–2.15)	0.32	1.19 (0.68–2.07)	.53	
CD163+ to CD8+	0.92 (0.57–1.46)	.72	1.32 (0.80–2.19)	.26	0.94 (0.56–1.57)	0.82	1.46 (0.83–2.55)	.18	
Average number in 100 μm ^a									
CD8+ to CD163+	0.57 (0.35–0.92)	.023 ^b	0.64 (0.36–1.12)	.12	0.55 (0.32–0.93)	0.02 ^b	0.73 (0.41–1.30)	.29	
CD163+ to CD8+	2.03 (1.24–3.30)	.004 ^b	1.63 (0.97–2.75)	.06	2.28 (1.33–3.91)	0.003 ^b	1.69 (0.96–2.97)	.06	
Proximity in 0–20 μm radius ^a									
CD8+ to CD163+	0.80 (0.50–1.28)	.35	0.87 (0.53–1.43)	.60	0.74 (0.44–1.23)	0.25	0.78 (0.46–1.32)	.36	
CD163+ to CD8+	1.15 (0.72–1.83)	.55	1.03 (0.62–1.70)	.89	1.07 (0.64–1.79)	0.76	1.03 (0.60–1.76)	.89	

^a All parameters are evaluated using high vs low contrast (for average distance high as reference [higher distance], whereas for other parameters low as reference [less density-proximity]). Multivariable models adjusted for Breslow thickness, ulceration, mitotic rate, and sentinel lymph node.
^b Statistically significant.

tendency of a favorable role of CD8+ cells in patient outcomes. Here, we used a more precise digital quantitation of the spatial proximity distribution and relative distance of tumor and immune cells to predict prognosis in primary CM patients, identifying patients at a high risk of disease recurrence. We investigated the spatial proximity distribution of CD8+TILs and CD163+ TAMs and SOX10+ tumor cells in biopsies from patients with primary CM. Although proximity distribution analysis was an approximation of cellular interactions, recently published proximity data^{11,19} suggested the utility and the potentiality of analyzing spatial proximity distribution of immune cells within SOX10+ tumor cells in primary CM. Indeed, our results showed that the absolute density measure did not mirror the proximity results, indicating that proximity and absolute intratumoral density should be both evaluated to provide a comprehensive assessment of the tumoral microenvironment.

Gartrell et al¹¹ demonstrated that high density of CD8+ TILs, particularly in the stroma, was a favorable indicator, and CD8+ TILs close spatial proximity to nonproliferating tumor (Ki67-) cells was correlated with positive patient outcomes. More recently, an evaluation of CD8+ T cell phenotypes has shown that high levels of CD39+CD103+PD-1-CD8+ T cells were associated with improved outcomes for primary CM patients and that the close proximity of this CD8+ T cell phenotype to tumor cells were also closely associated with reduced melanoma recurrence.

Our data are in line with the previous findings, by assessing the proximity using a radius cutoff of 0–20 μm,²² we observed a prognostic role of CD8+ cells in primary CM. Patients with SOX10+ cells with high proximity to CD8+ TILs in 20 μm radius had longer DFS and OS. Furthermore, in combined analyses, OS was increased in primary CM patients with SOX10+ melanoma cells with high proximity to CD8+ TILs/low proximity to CD163+ TAMs in a 20 μm radius compared with melanoma patients with SOX10+ tumor cells with low proximity to CD8+ TILs/high proximity to CD163+ TAMs in both univariate and multivariate models, demonstrating that TILs and TAMs are both involved. Moreover, it was already demonstrated that also the indirect proximity between TILs and TAMs can influence prognosis in primary CM patients.¹¹ Close proximity of CD8+ TILs to HLA-DR- TAMs was associated with poor survival in primary CM.¹¹ We demonstrated that DFS and OS were influenced by the average number of CD8+ TILs within a 100-μm radius from CD163+ TAMs and vice versa.

M2 macrophage phenotype (CD163+ cells) promotes tumor growth by releasing growth factors that favor cell proliferation^{24,25}

and CD8+ cell exhaustion.²⁵ However, despite this, CD8+ cells in close contact with malignant cells reduce tumor progression.¹⁹ In this context, our data suggested again the role of M2 TAMs in reducing the favorable action of CD8+ TILs and the role of CD8+ cells in limiting the disadvantageous action of CD163+ cells in primary CM patients.

Interestingly, when we evaluated separately SLN-positive and SLN-negative patients, we found that in SLN-negative patients, high proximity of CD8+ cells to CD163+ cells has a positive impact on DFS and OS, whereas high proximity of CD163+cells to CD8+ cells has a significant negative impact on DFS and OS in SLN-negative patients. These findings could help identify high-risk patients in the context of thick melanoma and a negative SLN.

Our study has some strengths and limitations. First, we performed 3 different proximity analyses to better explore TME and exploratively investigated different approaches to proximity distribution among different cells. Furthermore, all analyses were replicated on SNL+ or SNL- patients, and indirect proximity between immune cells was deeply and extensively investigated. In addition, the use of brightfield triple immunostain (SOX10/CD8/CD163 multiplex protocol) and evaluation of whole stains instead of tissue microarrays allows optimal correlation with morphology. Possible limitations of the study are the following: (i) our patient cohort include only primary CM with a Breslow thickness of >2 mm and represents a relatively small study series with unknown SLN status in 21 cases. Moreover, a priori calculation of the sample size or at least its justification can provide robustness to the survival analyses; (ii) tumor samples include 6 Acral Melanoma and 1 Lentigo Maligna Melanoma, and this reduces the homogeneity of our patient cohort; (iii) lack of validation in an external independent cohort; (iv) a larger panel of immunostains may be needed to dissect TME complexity and its influence of TME on patient outcomes; and (v) cells located near the tissue boundaries promote an edge effect; however, additional analyses, such as image padding, interpolation, and statistical correction, can improve the accuracy of the image analysis cell count. Additionally, the lack of data regarding clinical treatments may be a bias for the survival analysis.

In conclusion, the current study assessed the role of the relative spatial proximity distribution of melanoma cells and CD8+ TILs and CD163+ TAMs cells and their prognostic effect in primary CM patients via multiplex brightfield IHC. Our study underlines the importance of quantifying not only the absolute density of

Average number within 100µm

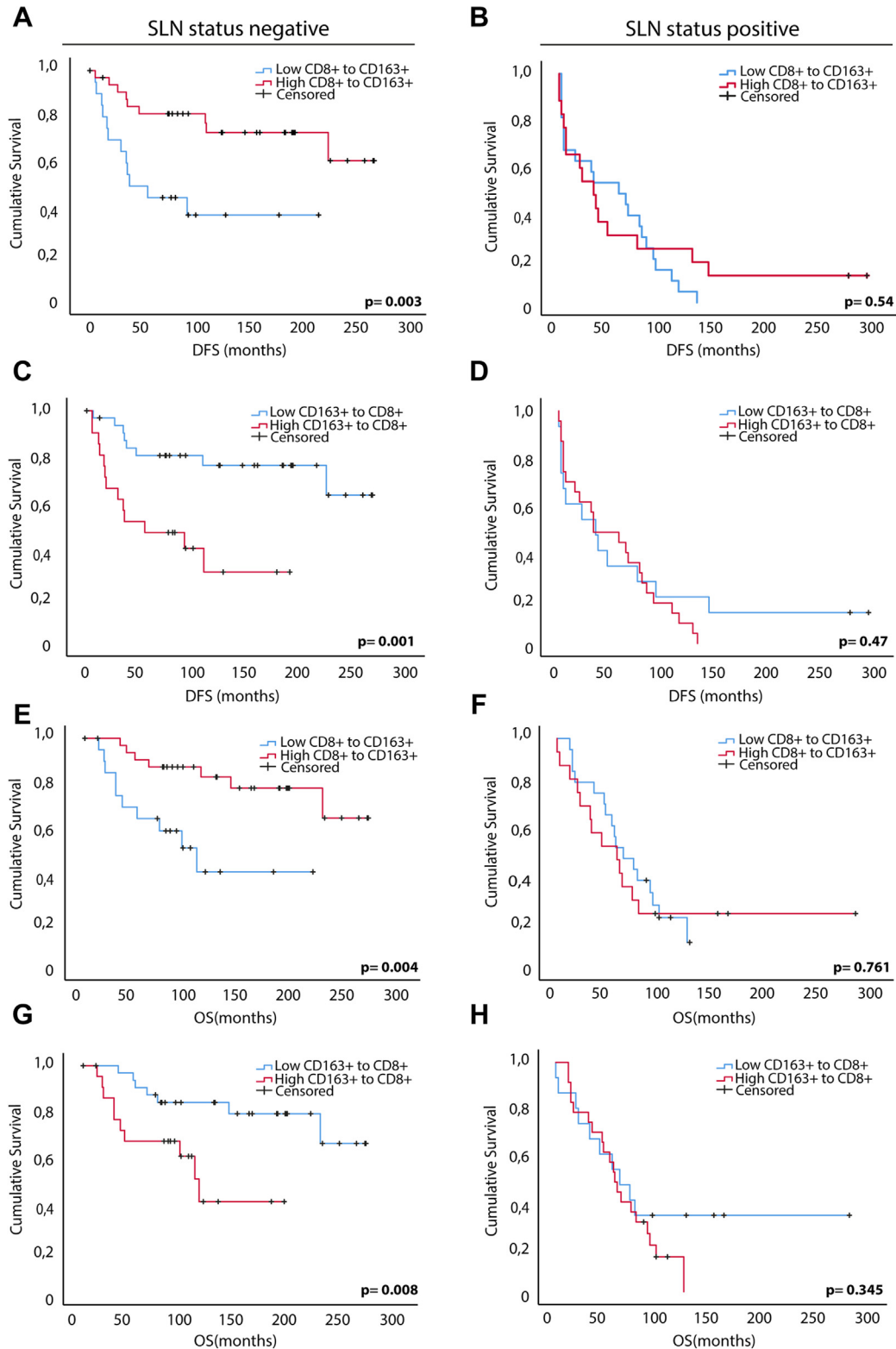


Figure 4.

Separate subgroup analysis in SLN-positive and SLN-negative groups of average number within 100 µm. Crude Kaplan–Meier survival analyses of CD8+ to CD163+ average number within 100 µm (A, E) (log-rank $\chi^2 = 8.81$, $P = .003$ and log-rank $\chi^2 = 8.50$, $P = .004$, respectively) or CD163+ to CD8+ average number within 100 µm (C, G) (log-rank $\chi^2 = 10.54$, $P = .001$ and log-rank $\chi^2 = 6.98$, $P = .008$, respectively) in SLN-negative group. Crude Kaplan–Meier survival analyses of CD8+ to CD163+ average number within 100 µm (B, F) (log-rank $\chi^2 = 0.37$, $P = .54$ and log-rank $\chi^2 = 0.09$, $P = .761$, respectively) or CD163+ to CD8+ average number within 100 µm (D, H) (log-rank $\chi^2 = 0.51$, $P = .47$ and log-rank $\chi^2 = 0.89$, $P = .345$, respectively) in SLN-positive group. Patients were divided into the high- and low-proximity groups, based on the median values, respectively. P values reflect the comparisons between 2 groups by univariate analysis using the log-rank test.

immune cells but also the individual and combined relative spatial proximity distributions and distances.

Author Contributions

D.M., M.M., and F.D.L. performed study concept and design, results interpretation, and review and revision of the paper; F.U., F.D.L., and L.F.I. wrote the first draft of the manuscript; S.S. and V.M. provided data collection and annotation; F.U. and S.S. carried out the experiments with D.M. supervision; L.F.I. provided statistical analysis of data; and V.G., A.M.G., C.M., A.C., G.P., and M.M. provided clinical data. All authors read and approved the final paper.

Data Availability

The datasets used and analyzed during the current study are available from the corresponding author on reasonable request.

Funding

This work was funded by the Associazione Italiana per la Ricerca sul Cancro - AIRC "Programma di ricerca 5 per Mille 2018—ID#21073."

Declaration of Competing Interest

The authors declare no competing interest.

Ethics Approval and Consent to Participate

Approval to conduct the study was obtained from the local Ethics Committees of the participating centers. Specifically, the use of FFPE sections of human samples was approved by the Local Ethics Committee (13676_bio, protocol Id.21073) according to the Helsinki Declaration, and informed consent was obtained.

Supplementary Material

The online version contains supplementary material available at <https://doi.org/10.1016/j.labinv.2023.100259>

References

1. Leiter U, Eigentler T, Garbe C. Epidemiology of skin cancer. *Adv Exp Med Biol.* 2014;810:120–140.
2. Ding L, Gosh A, Lee DJ, et al. Prognostic biomarkers of cutaneous melanoma. *Photodermatol Photoimmunol Photomed.* 2022;38:418–434.

3. Gershenwald JE, Scolyer RA, Hess KR, et al. Melanoma staging: evidence-based changes in the American Joint Committee on Cancer eighth edition cancer staging manual. *CA Cancer J Clin.* 2017;67:472–492.
4. Attrill GH, Ferguson PM, Palendira U, et al. The tumour immune landscape and its implications in cutaneous melanoma. *Pigment Cell Melanoma Res.* 2021;34:529–549.
5. Clemente CG, Mihm MC, Bufalino R, et al. Prognostic value of tumor infiltrating lymphocytes in the vertical growth phase of primary cutaneous melanoma. *Cancer.* 1996;77:1303–1310.
6. Azimi F, Scolyer RA, Rumcheva P, et al. Tumor-infiltrating lymphocyte grade is an independent predictor of sentinel lymph node status and survival in patients with cutaneous melanoma. *J Clin Oncol.* 2012;30:2678–2683.
7. Thomas NE, Busam KJ, From L, et al. Tumor-infiltrating lymphocyte grade in primary melanomas is independently associated with melanoma-specific survival in the population-based genes, environment and melanoma study. *J Clin Oncol.* 2013;31:4252–4259.
8. Schatton T, Scolyer RA, Thompson JF, et al. Tumor-infiltrating lymphocytes and their significance in melanoma prognosis. *Methods Mol Biol.* 2014;1102:287–324.
9. Mihm MC, Mulé JJ. Reflections on the Histopathology of Tumor-Infiltrating Lymphocytes in Melanoma and the Host Immune Response. *Cancer Immunol Res.* 2015;3:827–835.
10. Piras F, Colombari R, Minerba L, et al. The predictive value of CD8, CD4, CD68 and human leukocyte antigen-D-related cells in the prognosis of cutaneous malignant melanoma with vertical growth phase. *Cancer.* 2005;104:1246–1254.
11. Gartrell RD, Marks DK, Hart TD, et al. Quantitative analysis of immune infiltrates in primary Melanoma. *Cancer Immunol Res.* 2018;6:481–493.
12. De Logu F, Galli F, Nassini R, et al. Digital immunophenotyping predicts disease free and overall survival in early stage melanoma patients. *Cells.* 2021;10:1–20.
13. Allavena P, Sica A, Solinas G, et al. The inflammatory micro-environment in tumor progression: the role of tumor-associated macrophages. *Crit Rev Oncol Hematol.* 2008;66:1–9.
14. Jensen TO, Schmidt H, Møller HJ, et al. Macrophage markers in serum and tumor have prognostic impact in American joint committee on cancer stage I/II melanoma. *J Clin Oncol.* 2009;27:3330–3337.
15. Tremble LF, McCabe M, Walker SP, et al. Differential association of CD68+ and CD163+ macrophages with macrophage enzymes, whole tumour gene expression and overall survival in advanced melanoma. *Br J Cancer.* 2020;123:1553–1561.
16. Falleni M, Savi F, Tosi D, et al. M1 and M2 macrophages' clinicopathological significance in cutaneous melanoma. *Melanoma Res.* 2017;27:200–210.
17. Salmi S, Siiskonen H, Sironen R, et al. The number and localization of CD68+ and CD163+ macrophages in different stages of cutaneous melanoma. *Melanoma Res.* 2019;29:237–247.
18. Stack EC, Wang C, Roman KA, et al. Multiplexed immunohistochemistry, imaging, and quantitation: a review, with an assessment of Tyramide signal amplification, multispectral imaging and multiplex analysis. *Methods.* 2014;70:46–58.
19. Attrill GH, Lee H, Tasker AT, et al. Detailed spatial immunophenotyping of primary melanomas reveals immune cell subpopulations associated with patient outcome. *Front Immunol.* 2022;13:1–16.
20. Ugolini F, Pasqualini E, Simi S, et al. Bright-Field Multiplex Immunohistochemistry Assay for Tumor Microenvironment Evaluation in Melanoma Tissues. *Cancers (Basel).* 2022;14. <https://doi.org/10.3390/CANCERS14153682>
21. Gide TN, Silva IP, Quek C, et al. Close proximity of immune and tumor cells underlies response to anti-PD-1 based therapies in metastatic melanoma patients. *Oncoimmunology.* 2020;9(1):1659093.
22. Sorensen T. A Method of establishing groups of equal amplitude in plant sociology based on similarity of species and its application to analyses of the vegetation on Danish commons. *Kongelige Danske Videnskabernes Selskab.* 1948;5:1–34.
23. Zheng X, Weigert A, Reu S, et al. Spatial density and distribution of tumor-associated macrophages predict survival in non-small cell lung carcinoma. *Cancer Res.* 2020;80:4414–4425.
24. Wynn TA, Chawla A, Pollard JW. Macrophage biology in development, homeostasis and disease. *Nature.* 2013;496:445–455.
25. Christofides A, Strauss L, Yeo A, et al. The complex role of tumor-infiltrating macrophages. *Nat Immunol.* 2022;23:1148–1156.